ELSEVIER

Powder Technology 105 (1999) 30–38

POWDER TECHNOLOGY

www.elsevier.com/locate/powtec

Lab-scale roller table mill for investigating the grinding behaviour of coal

Volkmar Werner, Jacek Żelkowski, Klaus Schönert *

Institute for Energy Process Engineering and Fuel Technology and Institute of Mineral Processing, University Clausthal, Erzstraße 18, D-38678 Clausthal-Zellerfeld, Germany

Abstract

The test mill is equipped with one roller. The material bed can be discharged completely after overrolling. Grinding force, torque and gap width are measured. Cycle tests with three coals have been performed for simulating a closed circuit process. The grinding behaviour is characterized by the following relations: compaction of the particle bed and specific power draft vs. specific grinding force, production of fine material (dust), circuit factor, specific surface of the dust and specific work-input of the grinding circuit vs. specific power draft.

Résumé

Le broyeur à l'échelle du laboratoire est équipé d'un rouleau. Le lit de matériaux est totalement aspiré après chaque passage. La force de broyage, le moment de rotation et la largeur de fente sont mesurés. Des essais cycliques, ayant pour but la simulation d'un circuit de broyage, ont été réalisés sur trois houilles différentes. Le comportement au broyage est présenté selon les relations suivantes: compression du lit de matériaux et absorption d'énergie spécifique en fonction de la force de broyage spécifique; production des fines particules (poussière), facteur de récirculation, surface spécifique des poussières et travail spécifique de broyage d'un cycle en fonction de la puissance spécifique.

Keywords: Roller table mill; Grinding behaviour; Coal

1. Introduction

The grindability of coals is characterized by the well-established Hardgrove Index (HGI) [1]. Manufacturers warrant and operation diagrams refer to it. The advantage of this test is the simple procedure with a simple device, in which eight balls overroll 60 times a 50 g sample of the fraction 0.6/1.18 mm. The mass M_{75} of the produced fine material -75 μm determines the HGI according to the relation $\mathrm{HGI} = A + B\,(M_{75}/\mathrm{gram})$, A and B are parameters resulting by calibration with standardized materials. Based on the experiences that a monotonously increasing function (sometimes even a linear one) relates the throughput $\dot{M}$ to the HGI, $\dot{M}$ can be predicted depending on the coal dust fineness and the grinding force. Zeisel has developed a further test device in which the sample is stressed as in the Hardgrove tester. However, the power and the energy consumption can be determined by recording the torque [2].

Several papers deal with the comparison of different grindability tests, the accuracy of the predictions and the limitations (e.g., Refs. [3,4]). Furthermore, overrolling tests have been performed for investigating this particular stressing mode [5–7]. All these investigations show that fairly good predictions can be achieved if grindability numbers and functions, respectively, are related to a standard or to a material already comminuted with that particular mill type and then transferred to that mill. However, the conditions for transferring are not elaborated completely. Therefore, a project was started for additional investigations of the roller table mill process, including the construction of an instrumented test mill, the development of test procedures, compression tests and investigations with

* Corresponding author

0032-5910/99/$ - see front matter
PII: S0032-5910(99)00115-1

technical mills. This paper reports on first results with the test mill.

2. Experimental

2.1. Test device

The test device is designed like a roller table mill with, however, only one roller. Figs. 1 and 2 show a scheme and a sketch. The grinding table (1) is shaped like an annular trough and driven with the motor (2). The conical grinding roller (3) fits in the trough. The roller and its bearings are mounted at the lever system (4) with the spring (5). The adjustable stop (6) limits the lever movement so that a contact between roller and table can be avoided. The feeding system (7) consisting of a funnel and a shaft is mounted opposite to the roller. The distance between the trough bottom and the shaft outlet can be varied for controlling the feed flow. The tube (8) behind the roller serves for discharging the material by an air stream. The mill is instrumented with transducers for the torque (9), the grinding force (10) and the gap between roller and trough bottom (11). The design parameters are as follows: middle trough diameter 150 mm, trough width 42 mm, middle roller diameter 100 mm, roller width 40 mm, roller inclination 15°, maximum motor power 5.5 kW, table revolutions 5 to 150 min^{-1}, table circumferential speed at 75 mm radius 0.04 to 1.18 m/s, grinding force up to 3 kN, specific grinding force up to 0.75 N/mm^2, maximum vertical roller movement 5 mm.

2.2. Test procedures and evaluation

Before each test, the spring is strained up to a force somewhat smaller than the wanted grinding force. The

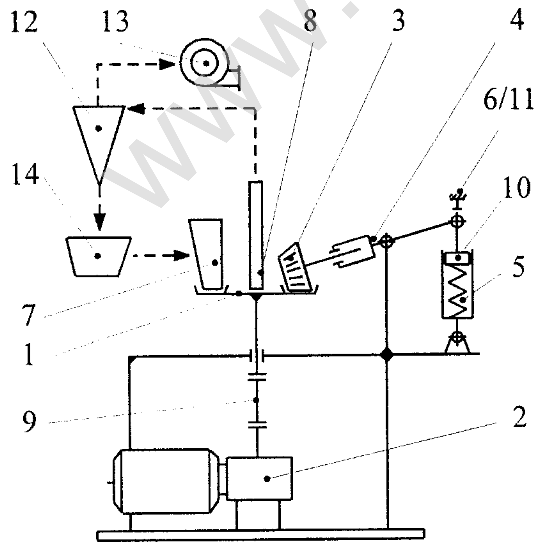

Fig. 1. Scheme of the test device.

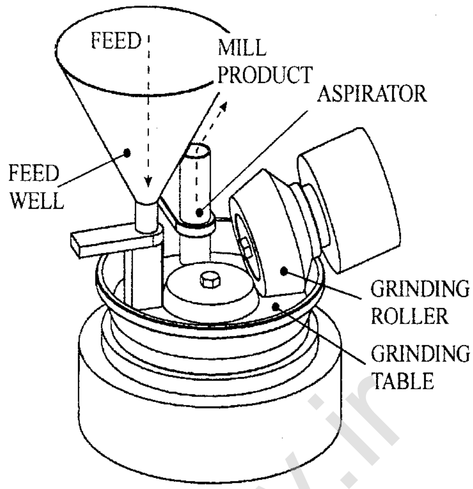

Fig. 2. Sketch of the test mill.

lever end contacts the stop. The entire material sample (200 to 1000 g) is filled into the funnel. The fan for discharging and the motor are started. The material bed lifts the roller, is compressed and discharged after being overrolled once. Because of the geometrical situation some material by-passes the roller. This fraction depends on the material flow behaviour (coal type, fineness, moisture), feed rate, table speed and grinding force. In the experiments discussed here, the by-pass counts 10 to 29%. The feed rate is adjusted with the distance between the feeding shaft and the trough bottom (bed height) and was varied between 3.3 and 4.1 g/s. Two types of experiments can be performed: overrolling and cycle tests. In the overrolling tests, the feed material is overrolled once and then analyzed. This can be repeated to study the development of the fineness as it depends on the energy expenditure. A cycle test enables to simulate the stationary state of a mill-classifier circuit. The procedure is that the mill product is sampled and then classified (here screening at 100 μm). The fine product is taken off, the coarse product mixed with fresh feed and this mixture ground again. The cycles are repeated up to the equilibrium, which was achieved after four to six cycles. In the test work discussed here, each cycle is accomplished with three overrollings to produce enough fine material for the classification.

Fig. 3 shows typical plots of an experiment; all the three parameters, torque, force and gap, are almost constant with small fluctuations.

In the following, the results are discussed with respect to:

- particle size distributions Q_F, Q_P, Q_C, Q_D in each cycle and in particular of the equilibrium cycle; indices F: mill feed, P: mill product, C: coarse product of classification (recirculating material), D: fine product of classification (dust)
- production of fine material f_x below a selected particle size x, here $x = 100$ μm, $f_x = Q_P(x) - Q_F(x)$

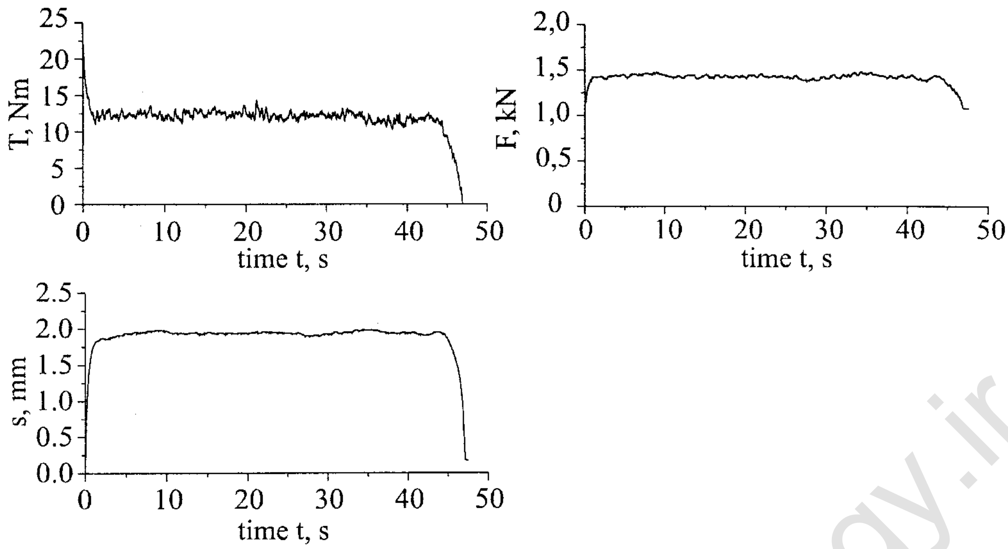

Fig. 3. Torque T, grinding force F and gap width s during overrolling.

– circuit factor k of the equilibrium cycle

$$k = (M_D + M_C)/M_D = M/M_D$$

M_D: fine product mass, M_C: coarse product mass, M: sample mass

– grinding force F or specific grinding force F_{sp}

$$F_{sp} = F/DL$$

D, L: diameter and width of the roller

– energy consumption E of a single overrolling

$$E = \int_0^t P(t')\,dt' \quad P(t) = 2\pi n T(t)$$

$$E = 2\pi n \int_0^t T(t')\,dt'$$

n: number of revolutions per minute, T: torque

– throughput related power draft P_M (specific power)

$$P_M = \overline{P}/\dot{M} = \int_0^t P(t')\,dt'/\dot{M}t = E/M$$

$\overline{P}$: average power, $\dot{M}$: mill throughput (including the by-pass material)

Table 1
Materials used

		Density ρ, g/cm^3	Ash (db), %	Volatile matter (daf), %	Moisture, %	Fraction -100 μm, %	HGI, °H
Westfalen	A	1.42	6.8	21.6	1.1	21	91
Prosper	B	1.41	8.4	35.4	2.7	18	46
Ibbenbüren	C	1.54	10.0	6.9	3.1	11	33

– specific surface S_M measured with the Blaine method [8]

– specific work-input W_M for grinding the sample to the dust product -100 μm in the equilibrium cycle, k: circuit factor

$$W_M = kP_M.$$

2.3. Materials

Three different German coals have been used, properties of which are listed in Table 1. The raw material was air-dried several days in the laboratory, then crushed and screened at 2 mm. Fig. 4 shows the particle size distributions.

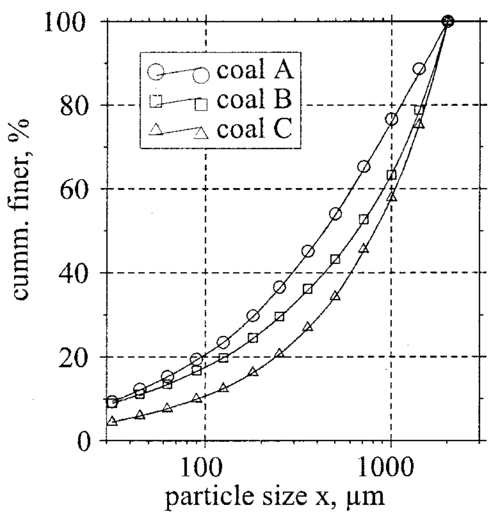

Fig. 4. Particle size distribution of used materials.

3. Results

3.1. Definition of the equilibrium cycle

The equilibrium is achieved if the size distributions do not change anymore in subsequent cycles. As an example, the results of coal C stressed with a specific force of 0.25 N/mm^2 should be discussed. The size distribution of the mill product, see Fig. 5, shifts step by step to the left and converges against a limiting curve, which is reached after the 5th cycle. Fig. 7 shows the mill feed and the mill product of the cycle 1, 3, 6 and demonstrates the influence of the feed size distribution. As known from earlier investigations, the size-reduction effect of interparticle breakage decreases and the size distribution of the fine material (dust) becomes somewhat coarser if the feed fineness rises (Fig. 6).

The experiments with the other coals and at other grinding forces have shown the same tendencies. Therefore, it was concluded to perform each test with six cycles and to take the average of the 5th and 6th cycle for representing the equilibrium, although the equilibrium can be achieved earlier with softer coals and higher forces.

3.2. Stressing situation

The stressing situation of a particle bed between roller and table can be characterized by parameters like the maximum pressure p_{max} upon the bed, the compaction angle α_0, the force acting angle β and the gap width s. Only the gap and the force acting angle can be determined in the test mill. For a general consideration s should be related to the roller diameter D. In coal mills this relative gap width is in the range between 0.005 and 0.025. Transferring this to the test mill, the gap should be between 0.5 and 2.5 mm. Fig. 8 shows that the measured gap widths lie in this range. As expected, s decreases with rising force.

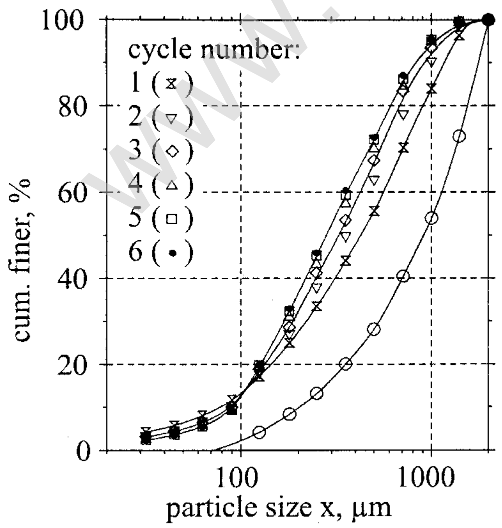

Fig. 5. Size distribution of the mill product after each cycle, coal C, $F_{sp} = 0.25$ N/mm^2.

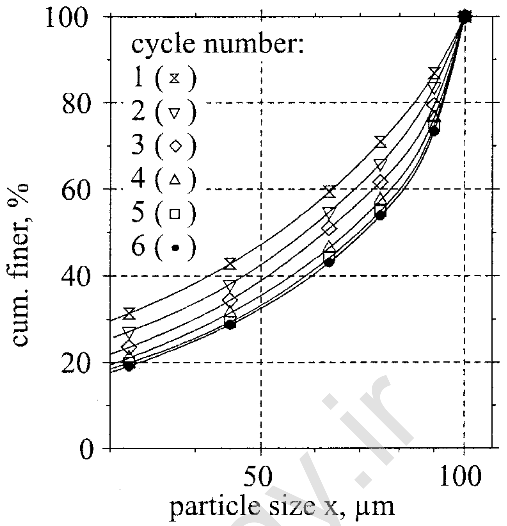

Fig. 6. Dust size distribution after each cycle, coal C, $F_{sp} = 0.25$ N/mm^2.

The gap width depends, firstly, on the introduction of the material into the gap due to the internal and external friction, secondly, on the specific milling force and, thirdly, on the material compactibility. The bed height after the funnel was always 4 mm. Different gap widths at the same specific force, therefore, indicate different amounts of by-passing material. The gap of the harder coal C is smaller than the gap of the softer coals A and B, this means C is introduced worse than A and B, the by-pass of C is bigger than the by-pass of A and B, C is more flowable than A and B. This corresponds to the experiences that the flowability increases with the hardness.

If the gap width is smaller than the maximum particle size, then the coarse particles are stressed by a direct contact between the table and the roller. In Table 2 the gap widths and the corresponding fractions of the mill feed coarser than s, $1 - Q_F(x = s)$, are listed. It can be seen that only at the test with coal C and $F_{sp} = 0.52$ N/mm^2 the direct contact stressing cannot be neglected.

The force acting angle β follows from the milling force F, the roller torque T_R and the roller diameter D. In the 1-roller test mill T_R is equal to the table torque T

$$\sin\beta \approx \beta = 2T/FD.$$

For a technical mill with N rollers usually the nominal force acting angle φ is determined with the table torque T, the average milling force $\overline{F}$ and the table diameter D_T according to:

$$\tan\varphi \approx \varphi = 2T/N\overline{F}D_T.$$

For comparing the test mill with technical mills the angle φ was calculated (see Fig. 9). With rising grinding force the angle φ decreases from about 10° to 5°, which is

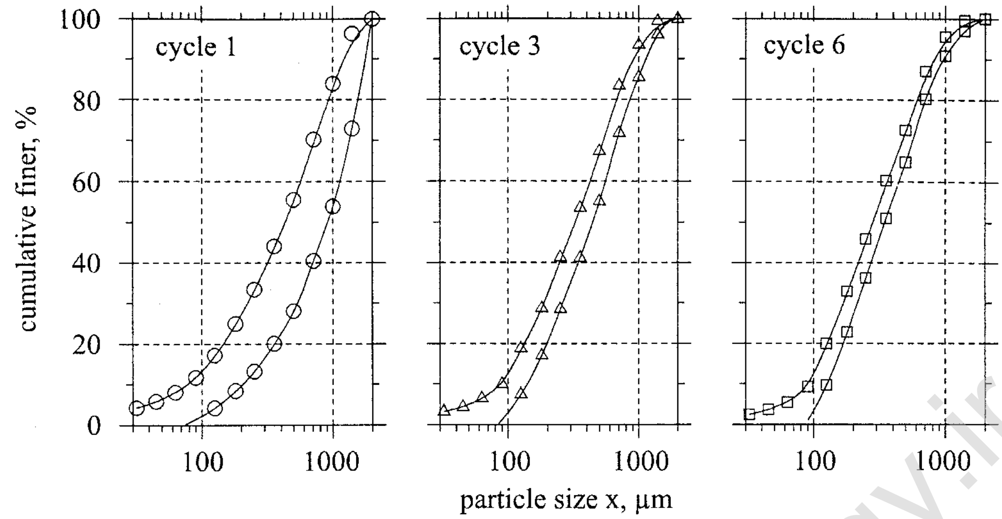

Fig. 7. Feed and product size distribution of cycle 1, 3 and 6, coal C, $F_{sp} = 0.25$ N/mm^2.

in the same range as evaluated for bigger mills. The angle does not depend strongly on the coal properties. The steeper curve for the softest coal A may be caused by overpressing this material which leads to a higher by-pass and a smaller angle. This point does not represent a proper performance.

For calculating the maximum pressure, the compaction angle and the pressure distribution in the compaction zone have to be known. In principle p_{max} can be expressed by

$$p_{max} = (F/DL)(1/I_F\,\alpha_0) = F_{sp}/I_F\,\alpha_0$$

with the dimensionless factor I_F depending only on the pressure distribution. As long as I_F and α_0 are unknown, only the specific force F_{sp} can be used as an indication for p_{max}. It may be mentioned here that roller table mills in power stations operate with F_{sp} between 0.10 and 0.50 N/mm^2.

The test mill runs with a circumferential speed of 0.036 m/s. This is comparable with that one of the Hardgrove tester (0.08 m/s), however, much slower than the velocity in technical coal mills of about 3 to 5 m/s. And the questions arise, whether and how the breakage and the material introduction into the gap depend on the speed. Investigations on interparticle breakage have shown that the stressing velocity within the range considered here does not influence the breakage of hard materials like quartz; however, the breakage of limestone as the size-reduction effect declines with increasing stressing velocity [9]. This strain rate effect is to be expected also for coal and has to be investigated. The speed influence on the introduction is well-known, because one of the most important demands for a proper operation refers to a stable material bed, which cannot be obtained above a critical speed. Below that limit the introduction is not affected much.

All above mentioned considerations leads to the conclusion that the stressing situation in the test mill is comparable with the one in a technical mill; however, the test mill may comminute somewhat better because of the low velocity. Probably, this does not affect the data transfer as long as ratios of grindability characteristics are used.

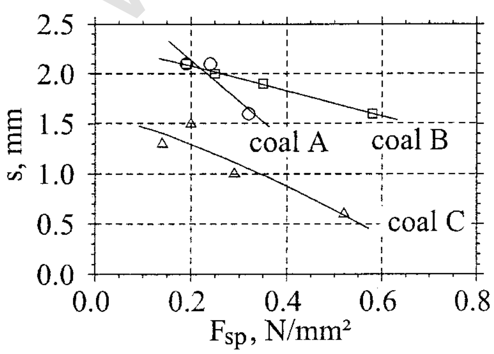

Fig. 8. Gap width s and specific grinding force F_{sp}.

3.3. Stressing intensity and size-reduction

The intensity of stressing a particle bed can be quantified by the pressure p upon it or by the energy consumed in one stressing event related to the volume or the mass

Table 2
Fraction of the mill feed coarser than gap width s

	Coal A			Coal B				Coal C			
F_{sp}, N/mm^2	0.19	0.24	0.32	0.19	0.25	0.35	0.58	0.14	0.20	0.29	0.52
s, mm	2.1	2.1	1.6	2.1	2.0	1.9	1.6	1.3	1.5	1.0	0.6
$1-Q_F$ $(x=s)$	0	0	0.02	0	0	0.06	0.03	0.05	0.03	0.08	0.24

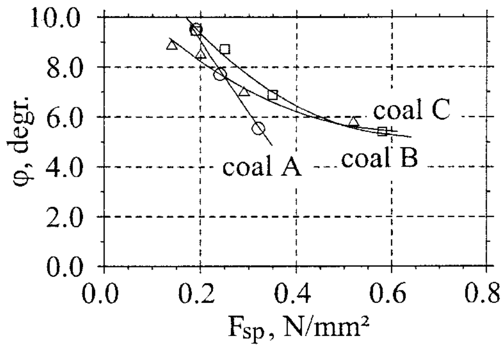

Fig. 9. Nominal force acting angle φ and specific grinding force F_{sp}.

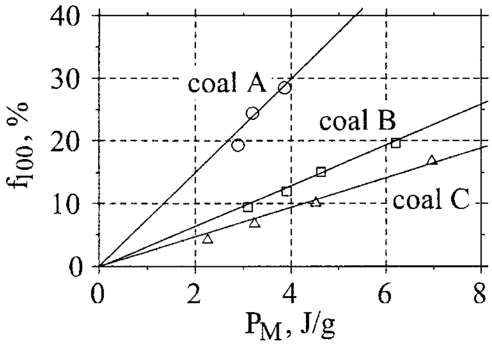

Fig. 11. Production of fine material -100 μm, f_{100}, and specific power P_M.

which is treated. This term is called the energy absorption E_M or E_V. Both these parameters p and E_V or E_M are related to each other, and it was shown that the size reduction effect in interparticle breakage can be better related to E_V or E_M than to p [9,10]. However, in a roller table mill both quantities cannot be determined; only the grinding force F, the power draft P and the mill throughput $\dot{M}$ are measurable. Based on these data, the specific grinding force $F_{sp} = F/DL$ and the specific power $P_M = P/\dot{M}$ can be calculated. P_M does not represent the energy absorption because $\dot{M}$ also includes the unstressed by-passing material. Therefore, E_M exceeds $(P/\dot{M})$ by the percentage of the by-pass, here about 20%. In Fig. 10 P_M is plotted over F_{sp}. At small forces P_M increases proportionally to F_{sp} and is not affected much by the coal properties. Then the curves bend slightly and branch with respect to the coal hardness as P_M increases with it. This is the typical tendency as known from other materials [11]. The P_M-values are in the range 1.0–2.3 J/g and the energy absorption can be assumed to be between 1.2 and 2.8 J/g. In preliminary compaction tests with a confined particle bed in a mold, the energy absorption is between 0.8 and 1.5 J/g at a pressure of 15 MPa. Therefore, the pressure in the test mill may be above this value. More experiments are planned to learn how compaction and overrolling tests can be linked to each other.

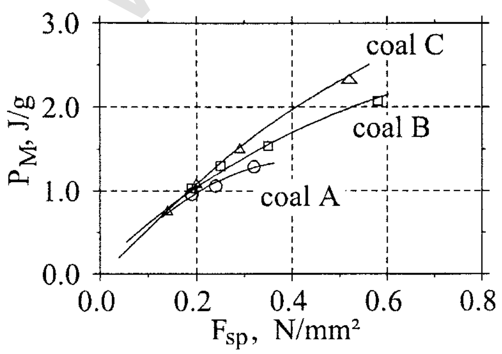

Fig. 10. Specific power P_M and specific grinding force F_{sp}.

Fig. 11 shows the production of fine material -100 μm, f_{100}, in the equilibrium cycle. Because the material is overrolled three times during one cycle, the specific power P_M is three times the values from Fig. 10. As expected, the coal influences strongly the results. They can be approximated with straight lines through the origin with slopes of 0.073, 0.032 and 0.024 g/J for coal A, B and C, respectively. The slopes can be considered as an indication for the grindability. The ratio of these slopes to the slope of a standard coal may express how much better or worse the particular coal can be ground. Using coal B for relating then the ratios are 2.28 for coal A and 0.75 for coal C. The corresponding ratios of the HGI-values of Table 1 are 1.98 and 0.72, respectively, and agree well.

3.4. Results from the equilibrium cycle

Fig. 12 shows the size distributions of the equilibrium cycle for the three coals stressed with $F_{sp} = 0.25$ N/mm^2. It can be seen that the mill feed distribution Q_F differs strongly from the distribution of the coal sample, which is due to the high recirculation of coarse material. Furthermore, the difference between the mill feed and the mill product distribution depends on the grindability of coal as it becomes less with decreasing HGI.

Fig. 13 demonstrates how the circuit factor k depends on the specific power P_M. Increasing P_M, which characterizes the stressing intensity, causes more comminution, therefore k decreases. The level of k and its P_M-sensitivity depend strongly on the coal hardness. The circuit factor declines from 5 to 3 for the softest coal A, from 9 to 4 for the moderate coal B and from 22 to 6 for the hardest coal C.

The size distribution of the dust becomes finer as the coal hardness decreases; the fractions below 32 μm are 47% (coal A), 37% (coal B) and 29% (coal C). An integral characterization of the dust fineness is given with the specific surface after Blaine (see Fig. 14). The influence of the stressing intensity, here expressed by P_M, becomes stronger as the coal hardness decreases.

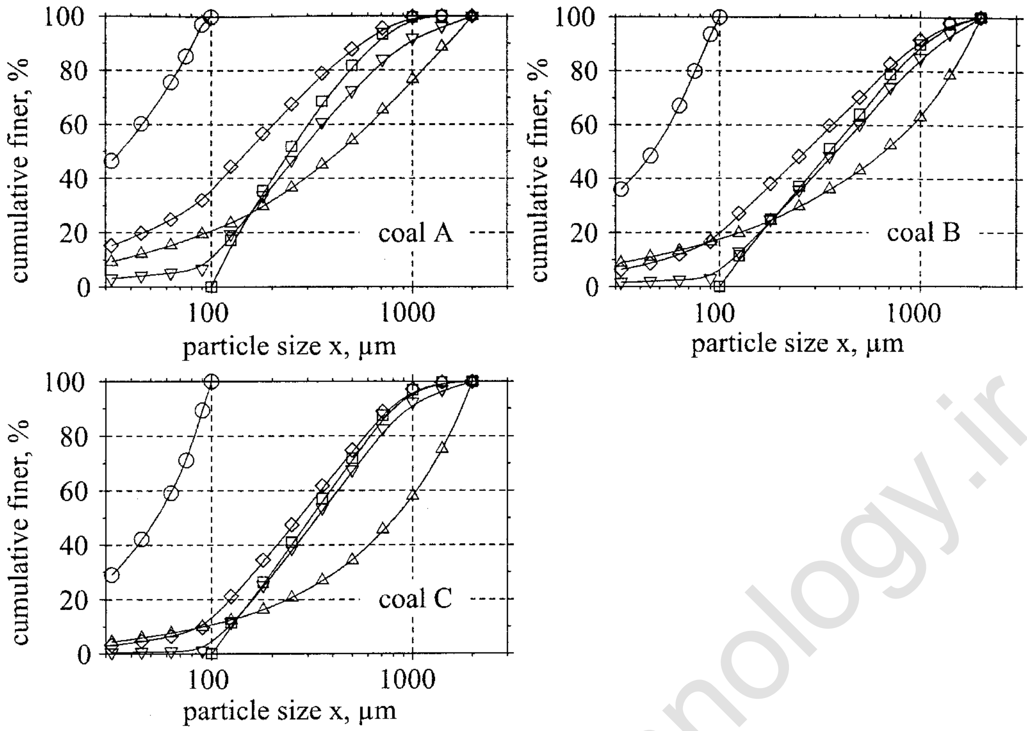

Fig. 12. Size distribution of the equilibrium cycle, $F_{sp} = 0.25$ N/mm^2, △ coal sample, ▽ mill feed, ◇ mill product, □ sieve oversize (grit), ○ sieve undersize (dust).

The equilibrium cycle represents a closed grinding process. Its specific work-input is given by $W_M = kP_M$; Fig. 15 shows W_M over the stressing intensity, here expressed with P_M. Only the hard coal C is affected somewhat as W_M declines from 13 to 10 kWh/t as P_M is increased from 1 to 7 J/g which is caused by increasing the specific grinding force from 0.15 to 0.52 N/mm^2. The reduction of the circuit factor from 22 to 5 overcompensates the higher P_M-value. The work-input of the two other coals is almost constant in the investigated range. Therefore, it is advantageous to increase the grinding force by which the mill capacity can be enlarged due to the decrease of the circuit factor. However, two conditions restrict the force: flake forming and bed instability.

In a view of comminution fundamentals, the energy utilization defined as the quotient of the produced specific surface divided by the specific work-input is of interest. These values are plotted in Fig. 16. As always found with other materials, e.g., quartz, cement clinker, limestone, the energy utilization declines with the stressing intensity [11]. This tendency can also be seen with coal. The level of $(\Delta S_M / W_M)$ depends on the coal properties and drops down as the coal becomes harder. Surprisingly, the three groups line up in such a way that they could be approximated with one curve. However, a one-line approximation

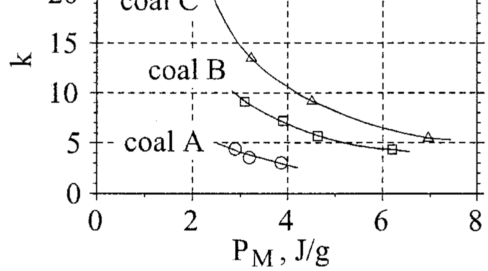

Fig. 13. Circuit factor k and specific power P_M.

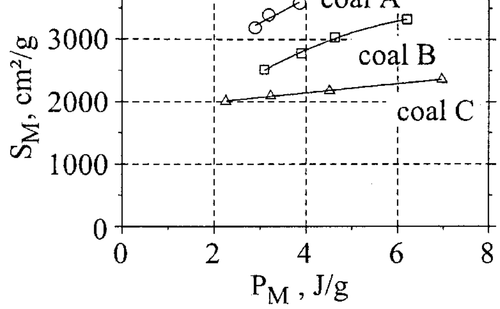

Fig. 14. Specific surface of the dust S_M after Blaine and specific power P_M.

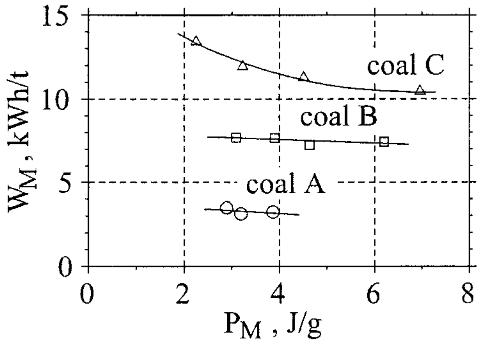

Fig. 15. Specific work-input W_M and specific power P_M.

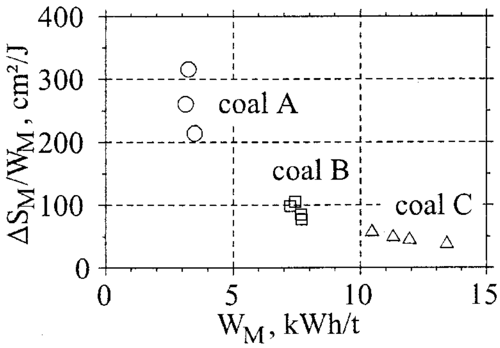

Fig. 16. Energy utilization $(\Delta S_M / W_M)$ and specific work-input W_M.

has to be proven with additional experiments using more coals of different properties.

4. Conclusions

The stressing situation in the test mill is comparable with the one in big roller table mills. All data describing the grinding characteristics, which are the production of the fine product (dust), the circuit factor, the size distribution of the dust and the specific work-input in the equilibrium cycle depend on the specific power draft in such a way as known with other materials. The term ''specific power draft'' is used here instead of the term ''energy absorption'' because a certain feed fraction by-passes the roller and remains unstressed. The energy absorption exceeds the specific power draft according to the percentage of the by-pass, which was measured to be in the range between 10 and 29%. The production of fine material increases proportional to the specific power draft at least within the investigated range. The slopes of these straight lines relate to each other almost like the HGI-ratios.

The question of how test mill data can be transferred to technical mills can only be answered seriously after a proper analysis of the roller table mill process with respect to the influence of the design and operational parameters. This will be discussed in another paper [12]. The throughput of a technical mill depends on the coal grindability, and it is usual to postulate that the throughput ratio of two different coals of type I and II is proportional of the ratio of their grindabilities. This proportionality is sometimes found, however, not always. Now the analysis of the roller mill process shows the conditions which have to be satisfied for this simple consideration; they are as follows:

1. The comminution in the particle size range of the test characterizes also the grinding behaviour of the coarser material.
2. The nominal force angle φ, which relates the grinding force F to the table torque T is the same for both materials.
3. The production of fine material (dust) f increases proportionally to the specific power draft P_M, and can, therefore, be expressed by $f = CP_M$.
4. The ratio of the slopes C_I / C_{II} of both coal types does not depend either on the wanted dust fineness or on the stressing velocity.
5. The fraction of by-passing material is almost the same for both materials as well in the test mill as in the technical mill.
6. The grade efficiency of the classifier is not affected by the coal type.

If all the above conditions are satisfied, then the said analysis leads to the throughput ratio $\dot{M}_I / \dot{M}_{II}$ as:

$$\dot{M}_I / \dot{M}_{II} = (C_I / C_{II})(F_{sp,I} / F_{sp,II}).$$

An agreement from experiences with this relation does not prove the satisfaction of all assumptions because some deviations could compensate each other, however, any deviation indicates that at least one assumption fails. Investigations with the test mill reported here help to better understand the complex roller table mill process since more data can be measured than with the Hardgrove tester.

Acknowledgements

This research was supported by the Bundesministerium für Wirtschaft via the Arbeitsgemeinschaft industrieller Forschungsvereinigungen (AiF). The authors are grateful for this financial help.

References

[1] R.M. Hardgrove, Transaction ASME 54 (1932) 37.
[2] H.G. Zeisel, Schriftenreihe der Zementindustrie, 1953, p. 31.
[3] R.L. Chandler, The British Coal Utilisation Research Association, Vol. 29, 1965, p. 333 and p. 371.
[4] U. Haese, P. Scheffler, H. Fasbender, Zement-Kalk-Gips 28 (1975) 316.
[5] G. Schwendig, Aufbereitungs-Technik 7 (1966) 489.

[6] G. Schwendig, Aufbereitungs-Technik 12 (1971) 550.
[7] N.J. Sligar, Tewksbury symposium of fracture 1979, Faculty of Engineering, Univ. Melbourne.
[8] DIN 66 126 (Teil 2), 1989.
[9] F. Müller, K. Schönert, in preprints 7th European Symposium Comminution 1990, Ljubljana, 1990, p. 179.
[10] K. Schönert, in: K.S.E. Forssberg, K. Schönert (Eds.), Comminution 1994, Elsevier, Amsterdam, 1996, p. 1.
[11] K. Schönert, Dissertation TH Karlsruhe, 1966.
[12] K. Schönert, in preparation.